Supplemental Information

A

Kinase	Labeling site	% Inhibition (%)
JNK1, JNK2, JNK3	Lys2	99.7
p38a	Lys2	16.4
p38a	Other	14.7
GSK3A	Lys2	20.4
GSK3B	Lys2	12.3
PFTAIRE1	Lys1	75.3
CDK9	Lys2	16.6
ROCK1	Other	-11.9
ROCK1, ROCK2	Lys2	-21.5
PIP5K3	ATP	91.8
PIK3C3	ATP	77.5
PIK3C3	ATP	74.2
PIP4K2C	ATP	77.2
PIP4K2C	ATP	84.3

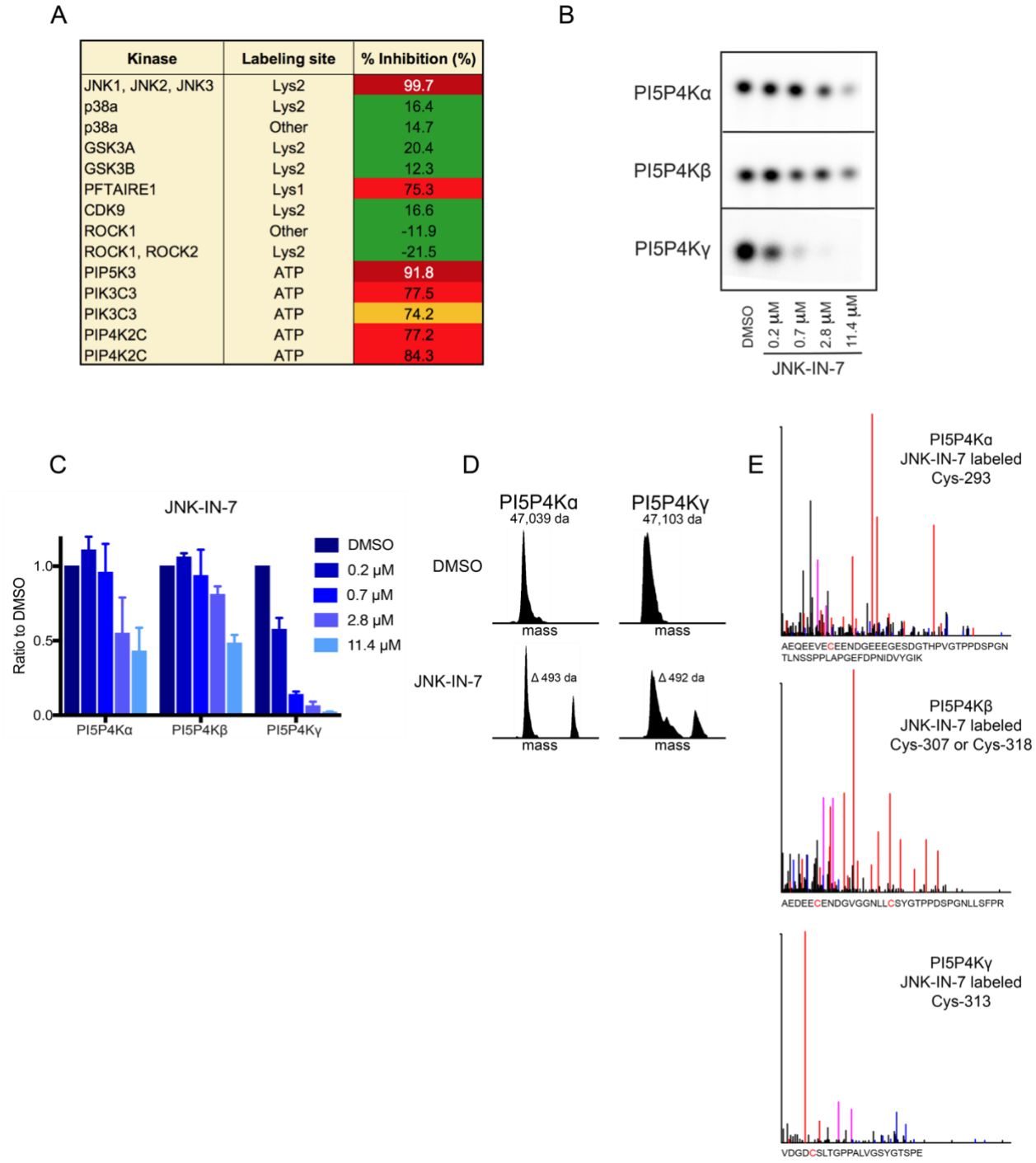

Figure S1, Related to Fig. 1A. (A) list of selected targets, including PI5P4Kγ (PIP4K2C), from KiNativ profiling of JNK-IN-7 at 1 μM for 3 hours in A375 cells. Full list is available in Zhang et al. (2012). (B) JNK-IN-7 inhibits kinase activity of all three PI5P4K isoforms in a radiometric TLC assay measuring radiolabeled PI-4,5-P_2. JNK-IN-7 was incubated with purified protein for 30min, followed by a 10min kinase reaction, quenching, lipid extraction and TLC development. (C) Quantification of (B). (D) Zero charge masses of recombinant PI5P4Kα and γ incubated with JNK-IN-7 for 2 hours at 37°C demonstrates covalent labeling of PI5P4K isoforms as determined by intact mass spectrometry. See Supplemental Intact MS Spectra for representative raw MS spectra used for charge deconvolution. (E) Subsequent protease digestion and tandem mass spectrometry confirms that THZ-P1-2 covalently labels cysteine residues on all three PI5P4K isoforms. The peptide for PI5P4Kβ was exclusively observed to be singly labeled at either Cys-307 or Cys-318. See Supplemental Intact MS Spectra for representative raw MS spectra used for charge deconvolution.

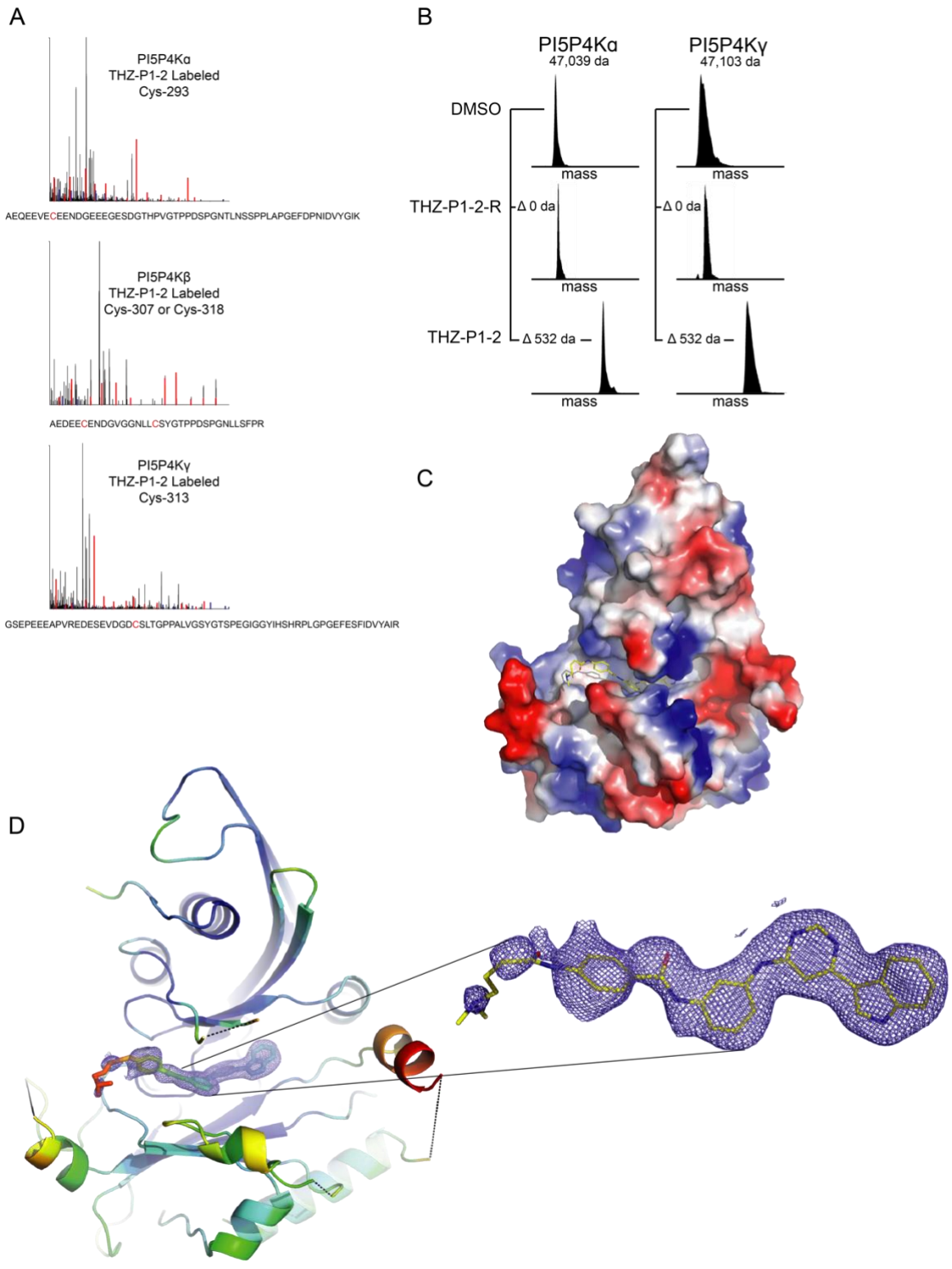

Figure S2, Related to Fig. 2. (A) Protease digestion and tandem mass spectrometry following intact mass labeling confirms that THZ-P1-2 covalently labels cysteine residues on all three PI5P4K isoforms. The peptide for PI5P4Kβ was exclusively observed to be singly labeled at either Cys-307 or Cys-318. Related to Fig. 2B. See Supplemental Intact MS Spectra for representative raw MS spectra used for charge deconvolution. (B) THZ-P1-2-R was found not to covalently label recombinant PI5P4Kα and γ when incubated with purified protein for 2 hours at 37°C. Mass labeling plot shown here is compared to mass shift observed with THZ-P1-2 from Fig. 2A. (C) Surface representation of co-crystal structure of PI5P4Kα in complex with THZ-P1-2. Related to Fig. 2C. (D) Zoom-in of ligand electron density within the active site of PI5P4Kα. See Table S1 for diffraction data collection and refinement statistics.

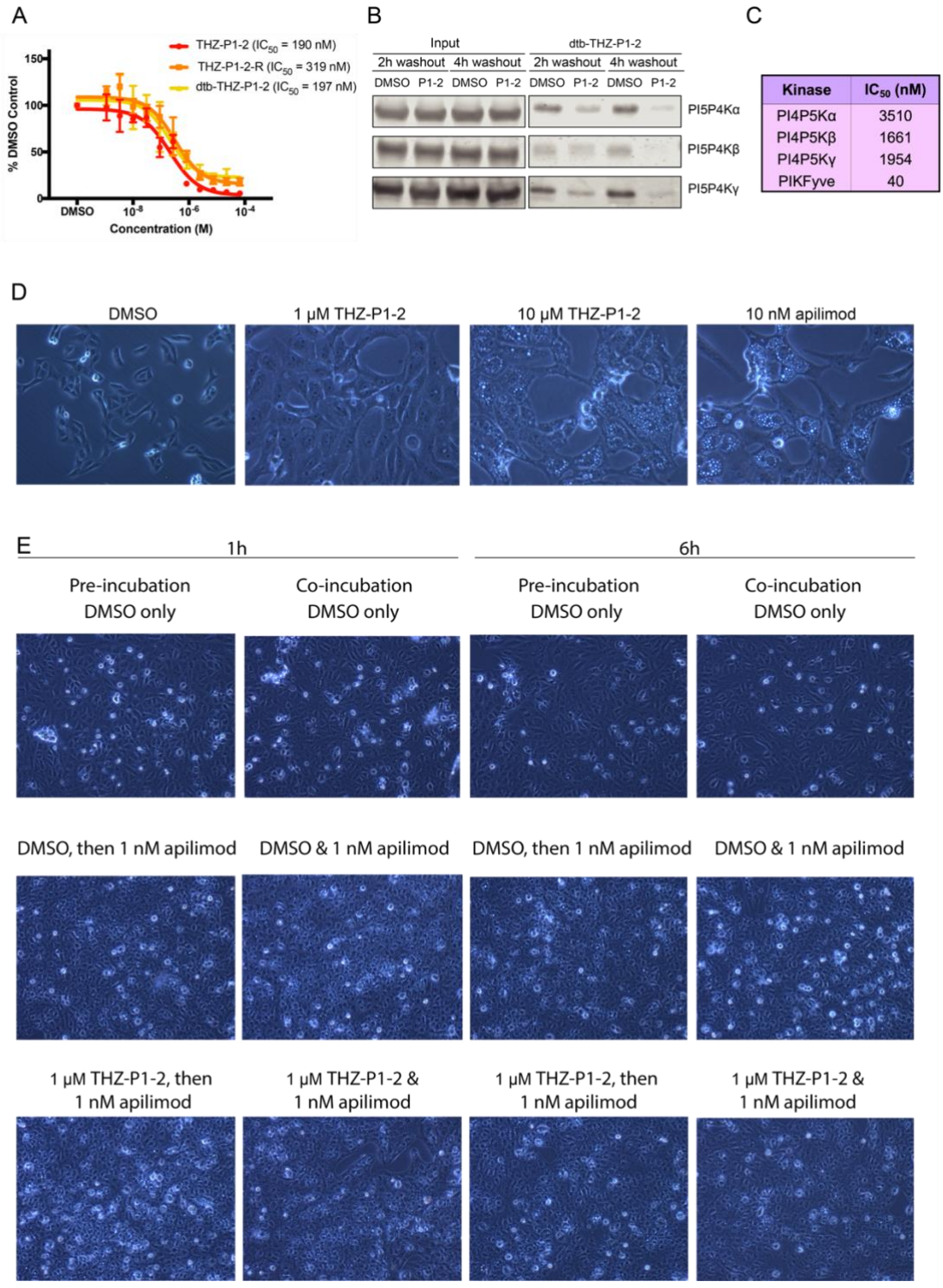

Figure S3, Related to Fig. 3. (A) THZ-P1-2-R and dtb-THZ-P1-2 were found to inhibit PI5P4Kα in an ADP-Glo assay, with a slight loss in potency with THZ-P1-2-R. Both compounds were incubated with PI5P4Kα for 15min before proceeding with a 1 hour reaction with ATP and development with ADP-Glo reagents. Data are represented as mean ± SEM. Plots are shown in comparison with THZ-P1-2 from Fig. 1B. (B) THZ-P1-2 engages PI5P4K isoforms at 2h and 4h timepoints, exhibiting prolonged engagement when a washout is performed. HEK293T cells were treated with DMSO or THZ-P1-2 at time, t=0 and cells were washed 2X with PBS at either 2 or 4h and harvested at the end of 6h. A streptavidin pulldown was then conducted in lysates after normalization of protein content with a BCA assay. (C) THZ-P1-2 inhibits the Type 1 PI4P5K kinases at a lower extent but shows potent inhibition on PIKfyve by ADP-Glo. *In vitro* kinase assays were performed by Invitrogen and Carna Biosciences. (D) THZ-P1-2 causes vacuolar enlargement, characteristic of PIKfyve inhibition, at a concentration of 10 μM but not 1 μM, compared to PIKfyve inhibitor apilimod at 10 nM treatment. Vero cells were treated with DMSO or compound for 6h and imaged. (E) Incubation of Vero cells with 1 μM THZ-P1-2 was unable to impair the PIKfyve inhibitory phenotype of apilimod. Preincubation: Vero cells were incubated with DMSO/THZ-P1-2 for 1 or 6h, washed with PBS to completely remove compound, treated with DMSO/apilimod and imaged after 6h. Coincubation: Vero cells were incubated with DMSO/THZ-P1-2 for 1 or 6h, and then co-treated with DMSO/apilimod and imaged after 6h.

A

Kinase	IC_{50} (nM)
ABL1	21.3
CSNK2A2	1340
KIT	>10000
PDGFRB	3050
RPS6KA4	>10000
TYK2	1600
BRK	313

B

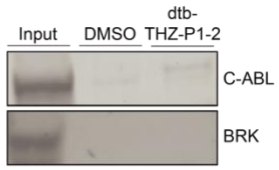

C

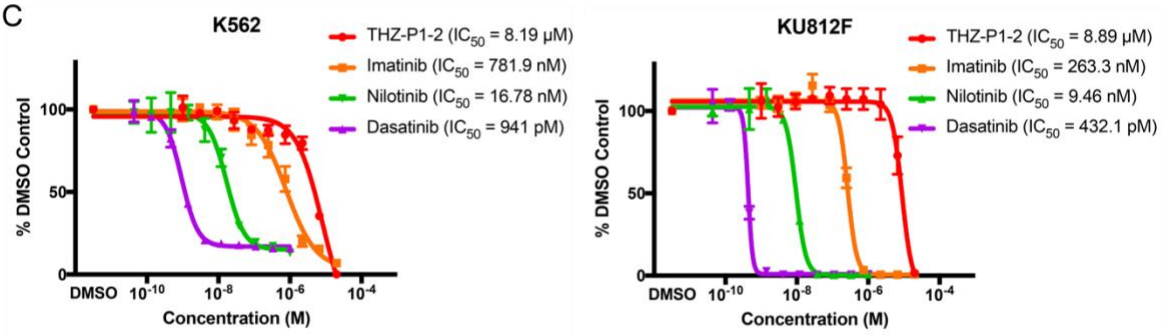

D

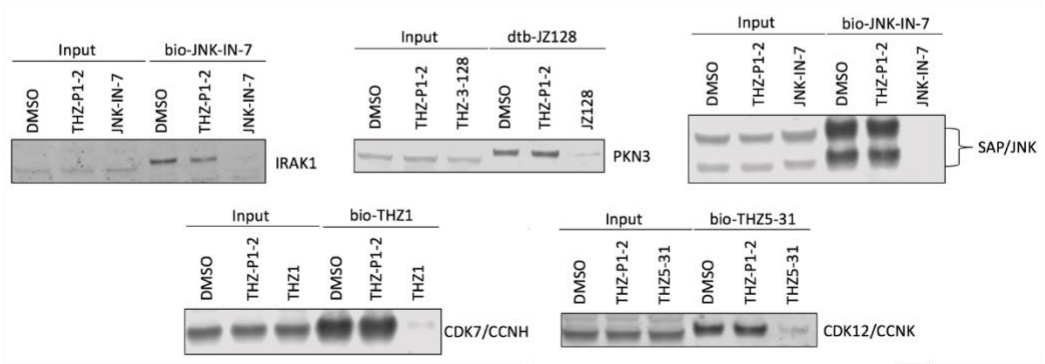

Figure S4, Related to Fig. 3 and 4. (A) THZ-P1-2 inhibits off-target kinases identified in the DiscoverX KINOMEScan panel to varying degrees. *In vitro* kinase assays were performed by Invitrogen using the Z'LYTE assay. (B) A streptavidin pulldown in HEK293T lysate shows little to no engagement of C-ABL and BRK by dtb-THZ-P1-2. (C) THZ-P1-2 shows mild antiproliferative activity on BCR-ABL addicted cell lines. Two cell lines containing BCR-ABL translocations, K562 and KU812F, were treated with THZ-P1-2 or known BCR-ABL inhibitors imatinib, nilotinib and dasatinib for 72h and assayed using Cell-Titer Glo. Data are represented as mean ± SEM. (D) THZ-P1-2 does not bind to and engage off-targets such as JNK, IRAK1, PKN3, CDK7 and CDK12 despite originating from the same core scaffold as inhibitors of these targets. Competitive streptavidin pulldowns in HEK293T cells were conducted with DMSO, 1 μM THZ-P1-2 and 1 μM of each target's corresponding inhibitor, followed by pulldown in lysate with 1 μM of the corresponding biotinylated or desthiobiotinylated inhibitor.

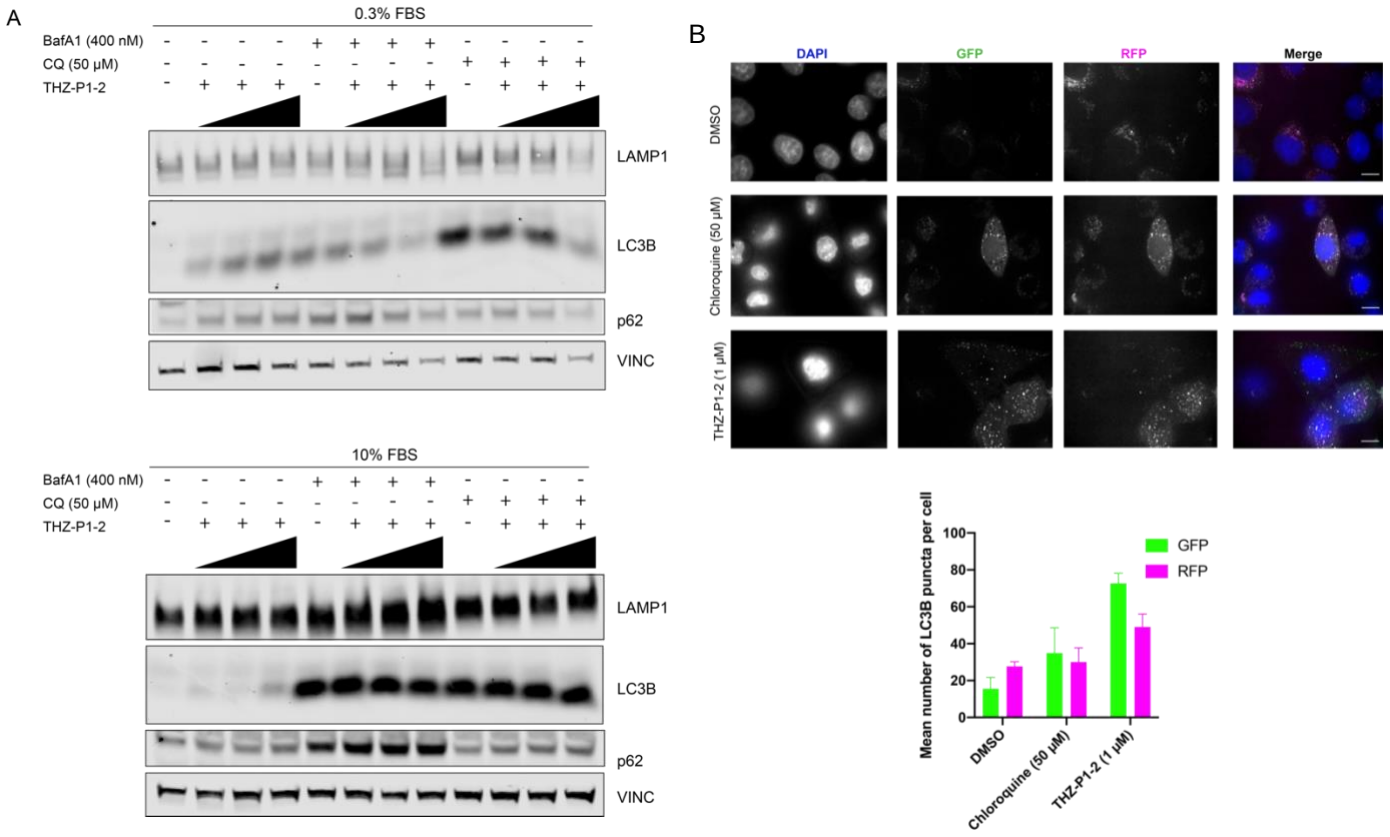

Figure S5, Related to Fig. 5. (A) THZ-P1-2 causes a slight increase in LAMP1, LC3B and p62 protein levels, as observed with positive control compounds bafilomycin A1 and chloroquine, and this effect is not cumulative in combination with these known autophagy inhibitors. HeLa cells were cultured for 24h in DMEM media supplemented with either 0.3% (serum-starved conditions) or 10% FBS. Cells were treated with DMSO, 250 nM, 500 nM, and 1000 nM concentrations of THZ-P1-2 and single doses of bafilomycin A1 and chloroquine, harvested after 24h, and analyzed by Western blot. Related to Fig. 5A. (B) THZ-P1-2 causes a dramatic increase in GFP signal and moderate increase in RFP signal in HeLa cells, as observed with positive control chloroquine, suggesting that autophagy was upregulated (leading to increase in LC3B fluorescence signal) but not completed with autolysosome fusion as GFP signal was not quenched. Cells were transfected with the Premo Autophagy Tandem Sensor for 16h and treated with DMSO or compounds for another 16h before analyzed using confocal microscopy. Fluorescence signal was quantified for at least n=10 per condition and data are represented as mean of two independent experiments ± SEM,

Scheme 1. Synthetic route of THZ-P1-2/THZ-1-2-R/dtb-THZ-P1-2[a], Related to Fig. 1A.

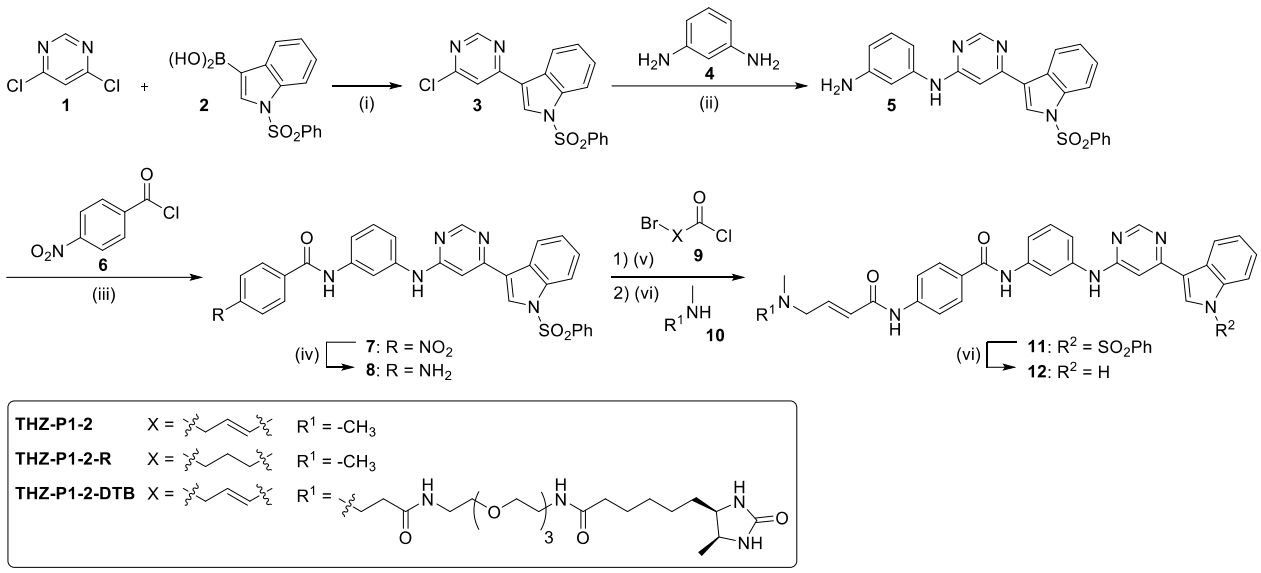

[a] Reagents and conditions: (i) $NaHCO_3$, $Pd(PPh_3)_2Cl_2$, ACN/H_2O (4:1, v/v), 90 °C, overnight, 61 % (ii) DIEA, NMP, 150 °C, overnight, 95 % (iii) pyridine, 80 °C, 3 h (iv) $SnCl_2 \cdot 2H_2O$, EtOAc/MeOH (5:2, v/v), 80 °C, overnight, 69 % over 2 steps (v) 1) DIEA, ACN, 0 °C, 5 min. 2) THF, rt, 2 h (vi) 1 m NaOH/1,4-dioxane (1:1, v/v), rt, 6 h, 7-73 % over 3 steps.

THZ-P1-2: MS m/z 532.24 $[M+H]^+$. ^1H NMR (400 MHz, DMSO-d_6) δ 11.73 (s, 1H), 10.50 (s, 1H), 10.19 (s, 1H), 9.55 (s, 1H), 8.63 (s, 1H), 8.27 (d, *J* = 7.2 Hz, 1H), 8.20 (s, 1H), 8.15 (d, *J* = 2.8 Hz, 1H), 8.00 (d, *J* = 8.7 Hz, 2H), 7.83 (d, *J* = 8.8 Hz, 2H), 7.59 – 7.44 (m, 2H), 7.37 (d, *J* = 8.3 Hz, 1H), 7.34 – 7.26 (m, 2H), 7.24 – 7.09 (m, 2H), 6.81 (dt, *J* = 15.4, 6.2 Hz, 1H), 6.40 (d, *J* = 15.4 Hz, 1H), 3.37 (d, *J* = 5.3 Hz, 2H), 2.39 (s, 6H).

THZ-P1-2-R: MS m/z 534.64 $[M+H]^+$. ^1H NMR (500 MHz, DMSO-d_6) δ 12.06 (s, 1H), 10.32 (s, 1H), 10.23 (s, 1H), 9.49 (s, 1H), 8.76 (s, 1H), 8.27 (d, *J* = 3.0 Hz, 1H), 8.24 (d, *J* = 2.1 Hz, 1H), 8.12 (d, *J* = 7.7 Hz, 1H), 7.97 (d, *J* = 8.6 Hz, 2H), 7.75 (d, *J* = 8.8 Hz, 2H), 7.56 (d, *J* = 7.7 Hz, 1H), 7.52 (d, *J* = 8.1 Hz, 1H), 7.43 (d, *J* = 8.2 Hz, 1H), 7.41 – 7.34 (m, 2H), 7.26 (p, *J* = 7.0 Hz, 2H), 3.16 – 3.04 (m, 2H), 2.81 (d, *J* = 4.6 Hz, 6H), 2.47 (d, *J* = 7.1 Hz, 2H), 2.02 – 1.90 (m, 2H).

dtb-THZ-P1-2 MS m/z 961.13 $[M+H]^+$. ^1H NMR (500 MHz, DMSO-d_6) δ 12.08 (s, 1H), 10.69 (s, 1H), 10.28 (s, 2H), 10.06 (s, 1H), 8.75 (s, 1H), 8.55 (s, 2H), 8.38 – 8.19 (m, 3H), 8.15 (d, *J* = 7.6 Hz, 1H), 8.00 (d, *J* = 8.8 Hz, 2H), 7.83 (d, *J* = 8.6 Hz, 2H), 7.54 (t, *J* = 8.6 Hz, 2H), 7.44 (d, *J* = 8.2 Hz, 1H), 7.40 – 7.32 (m, 2H), 7.32 – 7.15 (m, 2H), 6.83 (dt, *J* = 14.7, 7.2 Hz, 1H), 6.53 (d, *J* = 15.3 Hz, 1H), 3.69 – 3.56 (m, 4H), 3.52-3.49 (m, 8H), 3.43 (t, *J* = 6.0 Hz, 2H), 3.38 (t, *J* = 6.1 Hz, 2H), 3.25 (d, *J* = 7.0 Hz, 2H), 3.21 – 3.10 (m, 6H), 2.78 (s, 3H), 2.64 (t, *J* = 7.0 Hz, 2H), 2.05 (t, *J* = 7.5 Hz, 2H), 1.46 (q, *J* = 7.4 Hz, 2H), 1.28-1.22 (m, 4H), 0.95 (d, *J* = 6.4 Hz, 3H).

Table S1, Related to Figure 2C-D. Crystallization conditions, data collection and refinement statistics for co-crystal structure of complex THZ-P1-2 with PI5P4Kα.

Structure Name	**PI5P4Kα/THZ-P1-2**
Ligand	THZ-P1-2
RCSB accession code	6OSP
Data collection [a]	
Space group	$P2_1$
Cell dimensions	
a, *b*, *c* (Å)	44.19 98.68 105.12
a, b, g (°)	90.00 93.66 90.00
Resolution (Å)	44.1-2.21 (2.29-2.21) [b]
R_{pim}	0.042 (0.525)
$I / \sigma I$	13.44 (1.53)
Completeness (%)	99.17 (99.44)
Redundancy	3.7 (3.7)
Structure solution	
PDB entries used for molecular replacement	2YBX
Refinement	
Resolution (Å)	44.1-2.21
No. reflections	44717
R_{work} / R_{free}	0.1779/0.2254
No. atoms	5450
Protein	5102
Ligand/ion	92
Water	256
B-factors	
Protein	53.08
Ligand/ion	70.65
Water	50.74
R.m.s. deviations	
Bond lengths (Å)	0.012
Bond angles (°)	1.15
Ramachandran	
Preferred	98.21%
Allowed	1.63%
Not Allowed	0.16%

[a] A single crystal was used to collect data for each of the structures reported here.

[b] Values in parentheses are for highest-resolution shell.

Table S2, Related to Fig. 3C. Complete dataset for THZ-P1-2 kinome selectivity using the DiscoverX commercial profiling platform.

The kinome selectivity dataset for THZ-P1-2 is 11 pages and provided as a supplemental excel table.

Data S1. Supplemental Intact MS Spectra, Related to Fig. 2A, S1D, S2B.